NANO LETTERS

2008
Vol. 8, No. 7
1844-1852

# Fundamental Design Principles That Guide Induction of Helix upon Formation of Stable Peptide−Nanoparticle Complexes

**Patrik Nygren,[†] Martin Lundqvist,[‡] Klas Broo,[§] and Bengt-Harald Jonsson*,[||]**

*Division of Applied Physics, IFM, and Division of Molecular Biotechnology, Linköping University, SE-581 83 Linköping, Sweden, School of Chemistry and Chemical Biology, University College Dublin, Belfield, Dublin 4 Ireland, and Department of Occupational and Environmental Medicine, Sahlgrenska Academy at Göteborg University, Göteborg, Sweden*

*Received February 8, 2008; Revised Manuscript Received May 1, 2008*

## ABSTRACT

**We have shown that it is possible to design a peptide that has a very low helical content when free in solution but that adopts a well-defined helix when interacting with silica nanoparticles. From a systematic variation of the amino acid composition and distribution in designed peptides, it has been shown that the ability to form helical structure upon binding to the silica surface is dominated by two factors. First, the helical content is strongly correlated with the net positive charge on the side of the helix that interacts with the silica, and arginine residues are strongly favored over lysine residues in these positions. The second important factor is to have a high net negative charge on the side of the helix that faces the solution. Apparently, both attractive and repulsive electrostatic forces dominate the induction and stabilization of a bound helix. It is also evident that using amino acids that have high propensity to form helix in solution are also advantageous for the formation of helix on surfaces.**

**Introduction.** Efficient use of bionanoparticles in medical therapy, industrial processes, and as diagnostic tools requires means to induce and maintain functional conformations of peptides and proteins on their surfaces. The introduction of functionality into designed peptides was achieved earlier by Chmielewski and co-workers who designed a replicating peptide system in which the reactivity is under the control of pH or salt.[1,2] An efficient oxaloacetate decarboxylase was constructed by Benner and co-workers,[3] and a self-replicating peptide and an efficient catalytic synthetic peptide ligase was constructed by Ghadiri and co-workers.[4,5] DNA recognition modules, such as the basic region leucine zipper, are unfolded in solution but adopt a stable, ordered conformation upon interaction with DNA.[6] DeGrado and co-workers[7] have analyzed the leucine zipper proteins and suggested fundamental principles for the design of peptides that adopt a helical structure upon interaction with recognition sites in DNA.

In this context, it is also fundamental to construct functional nanosystems, for applications ranging from target drug delivery and medical imaging to catalysis in chemical synthesis, that are robust and have high stability. Due to their high stability and ease of handling, nanoparticles of silica are attractive candidates as first generation partners in the construction of functional nanocomplexes with proteins or peptides that self-assemble on the surface. However, it is well-known that proteins tend to deform upon binding to silica.[8−14] Notably, the distribution of charges on natural proteins is not optimized for a "lock and key" fit with the negative charges on the surface of silica. Hence, charged surfaces tend to deform the proteins upon binding and consequently, the biological functions of the proteins are often destroyed or their efficiency is lowered.[8,10,12−22] In a previous study, we have shown that it is possible to utilize the highly negatively charged silica surface and to design peptides that interact favorably with these charges, so that peptide adsorption to silica nanoparticles induced a helical structure (Figure 1).[23] Charged surfaces have later been used to induce helical structure in de novo designed peptides with such diverse substrates as self-assembled monolayer (SAM) clad gold nanoparticles[24] and hydroxyapatite.[25] The ability

* Corresponding author. E-mail: nalle@ifm.liu.se.
[†] Division of Applied Physics, IFM, Linköping University.
[‡] University College Dublin.
[§] Sahlgrenska Academy at Göteborg University.
[||] Division of Molecular Biotechnology, Linköping University.

10.1021/nl080386s CCC: $40.75 
**Published on Web 06/10/2008**

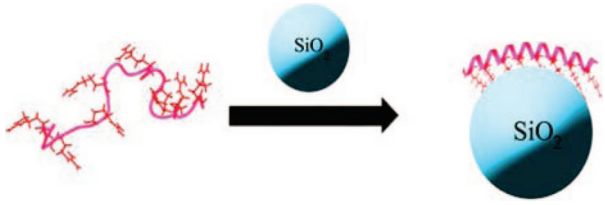


**Figure 1.** Schematic representation of surface induced helicity.

to generate a stable, well-defined structure on the surface of silica nanoparticles also presented the possibility of creating closely regulated systems with a variety of potential functionalities, which was demonstrated by the introduction of a catalytic site in one of the peptides.[23] In that study, a peptide was constructed using de novo design, which was unstructured in solution but "forced" to adopt a helical structure upon adsorption to silica nanoparticles. To ensure that it is the binding to the silica nanoparticles that causes the formation of helical structure, it is essential to incorporate a combination of positive and negative design elements, that is, that the design should strongly favor formation of a helical structure upon binding to the nanoparticles and strongly disfavor an ordered structure in solution. The electrostatic interactions (repulsive and attractive) are important for both positive and negative design. The present study investigates the properties of the peptide−nanoparticle system through a systematic variation of the design parameters. Thus, we have synthesized peptides to investigate the effects of (i) the density of positive charges, (ii) the spatial distribution of positive charges, (iii) the distribution of positive and negative charges for orientation of the helix on the surface, (iv) the role of amino acid helix propensities, and (v) the role of altering the size of the hydrophobic residues. In addition, we investigated the dependence of pH.

In the present study, 12 different peptides were designed in order to identify the various factors that contribute to formation of a helix on the surface of the silica nanoparticles and to quantify their relative importance.

(a) An initial assumption was that the interaction between the peptide and the silica surface might be dominated by electrostatic interactions between the negatively charged surface of the nanoparticle and a positively charged side of a helix. Therefore, arginine and lysine residues were incorporated in positions that would constitute one side of the induced helix. In the first construct (peptide 1), arginine was favored over lysine because of its guanidine group having a delocalized charge, high p$K_a$, and a low reactivity. At pH 9, the charge density on the helix and on the surface is of the same magnitude.[26] Besides being responsible for the peptide−surface interaction, the positive charges may also prevent the peptide from adopting a helical structure in solution due to electrostatic repulsion between the side chains, which occurs in the absence of appropriately spaced negative charges. The peptides 1, 2, 3, and 4 were synthesized to test the role of the density of positive charges and their spatial distribution, and peptide 5 was synthesized to compare the efficiency of lysine versus arginine.

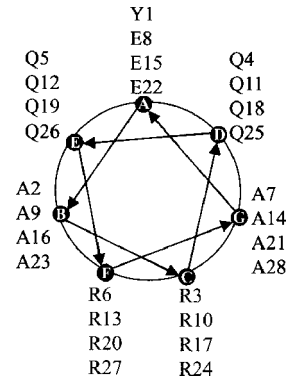


**Figure 2.** Amino acid sequence of peptide 1 depicted as a helical wheel. Each point gives rise to a row of amino acids, and each row is allocated a letter.

(b) In the design, rows A, D, and E (Figure 2) were directed away from the silica surface to face the solution. Therefore, polar residues were placed in rows D and E as their polar side chains would interact favorably with the solution. Polar residues with different propensities for formation of helix were tested in peptides 1 and 6. To further test the effect of the negatively charged silica surface on the formation of a helix, glutamic acid residues were incorporated in row A; that is, the glutamic acid carboxyl group might be repelled by the silica surface and would thereby assist the twist of the peptide backbone toward helical conformation. The importance of the total charge on the solution side of the helix was tested by altering the amino acid residues at positions A, D, and E by using peptides 1, 4, 7, 8, and 9.

(c) Positions B and G (Figure 2) were used to test the importance of hydrophobic residues of different sizes as well as different propensities to form a helix (peptides 1, 10, and 11).

The final goal was to construct a nanosystem in which the increase in helical content was optimized.

**Determination of Helical Content.** All peptides listed in Table 1 were investigated using near UV circular dichroism (CD) measurements (185−260 nm) at ∼0.1 mM concentration in pH 8.4, 9.0, and 9.8 in the presence and absence of nanoparticles. A typical result is illustrated by Figure 3, which shows CD spectra on peptide 1. The results suggest the formation of a pronounced helix upon the addition of nanoparticles, and a comparison of the spectra also indicates a significant dependence on pH. Notably, Lundqvist et al. have previously shown that the formation of a helix upon the addition of nanoparticles is due to binding of the peptide to the particle.[23] The helical content of the free peptides and the peptide nanoparticle complexes were calculated using CDSSTR[28–32] on all CD data, and the results are summarized in Table 2. The results presented in Table 2 clearly indicate that it is possible to optimize the design, as shown by the increase in helical content from 36% in the original design to 60% at pH 8.4, in the best construct. The importance of the different design elements is discussed in the following sections.

**Table 1.** Amino Acid Sequences of Peptide 1 to 12[a]

| Peptide | N-term | 1 | 2 | 3 | 4 | 5 | 6 | 7 | 8 | 9 | 10 | 11 | 12 | 13 | 14 | 15 | 16 | 17 | 18 | 19 | 20 | 21 | 22 | 23 | 24 | 25 | 26 | 27 | 28 | C-term |
|---|---|---|---|---|---|---|---|---|---|---|---|---|---|---|---|---|---|---|---|---|---|---|---|---|---|---|---|---|---|---|
| 1 | $CH_3CO$ | Y | A | R | Q | Q | R | A | E | A | R | Q | Q | R | A | E | A | R | Q | Q | R | A | E | A | R | Q | Q | R | C | $CONH_2$ |
| 2 | $CH_3CO$ | Y | A | R | Q | Q | N | A | E | A | R | Q | Q | N | A | E | A | R | Q | Q | N | A | E | A | R | Q | Q | N | A | $CONH_2$ |
| 3 | $CH_3CO$ | Y | A | R | Q | Q | N | A | E | A | N | Q | Q | R | A | E | A | R | Q | Q | N | A | E | A | N | Q | Q | R | A | $CONH_2$ |
| 4 | $CH_3CO$ | Y | R | R | Q | A | R | A | E | R | R | Q | A | R | A | E | R | R | Q | A | R | A | E | R | R | Q | A | R | A | $CONH_2$ |
| 5 | $CH_3CO$ | E | A | K | Q | Q | K | A | E | A | K | Q | Q | K | A | E | A | K | Q | Q | K | A | E | A | K | Q | Q | K | A | $CONH_2$ |
| 6 | $CH_3CO$ | Y | A | R | N | N | R | A | D | A | R | N | N | R | A | D | A | R | N | N | R | A | D | A | R | N | N | R | A | $CONH_2$ |
| 7 | $CH_3CO$ | E | A | R | Q | Q | R | A | K | A | R | K | K | R | A | K | A | R | Q | K | R | A | E | A | R | Q | Q | R | A | $CONH_2$ |
| 8 | $CH_3CO$ | Y | A | R | Q | Q | R | A | E | A | R | Q | Q | R | A | H | A | R | Q | K | R | A | E | A | R | Q | Q | R | A | $CONH_2$ |
| 9 | $CH_3CO$ | C | R | A | E | R | R | E | A | R | A | E | R | R | E | A | R | A | E | R | R | E | A | R | A | E | R | R | Y | $CONH_2$ |
| 10 | $CH_3CO$ | Y | V | R | Q | Q | R | V | E | V | R | Q | Q | R | V | E | V | R | Q | Q | R | V | E | V | R | Q | Q | R | V | $CONH_2$ |
| 11 | $CH_3CO$ | Y | L | R | Q | Q | R | L | E | L | R | Q | Q | R | L | E | L | R | Q | Q | R | L | E | L | R | Q | Q | R | L | $CONH_2$ |
| 12 | $CH_3CO$ | R | A | E | R | R | E | A | R | A | E | A | R | A | A | R | A | E | A | R | A | E | R | R | E | A | R | A | E | $CONH_2$ |

[a] Amino acids designed to interact with the surface are shaded with gray. Both the N and C terminal were capped; the N terminal with an acetic group and the C terminal as an amide.

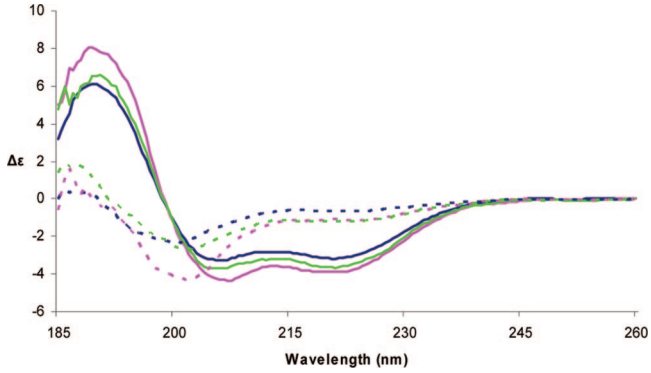


**Figure 3.** CD spectra for peptide 1. Blue, pink, and green represent pH 8.4, 9.0, and 9.8 respectively, with a solid line for samples with particles and a dashed line for samples without particles.

**Silica as Solid Support.** In this study, colloidal silica nanoparticles with a uniform (monodisperse) particle size of 9 nm diameter (corresponding to a surface area of 254 $nm^2$) have been used. They provide a negatively charged inorganic surface, and their size and transparency allow the use of conventional spectroscopic methods including far-UV CD to monitor the conformation of bound peptides. The surface charge density on these particles varies with pH and is around 0.5 $OH^-/nm^2$ at pH 8.4, 0.7 $OH^-/nm^2$ at pH 9, and 1.1 $OH^-/nm^2$ at pH 9.8. Furthermore, changing the curvature by use of nanoparticles with diameters of 6 and 15 nm had essentially no effect on the degree of helix, ±4% (data not shown), indicating that all silica surfaces with charge densities above 0.5 $OH^-/nm^2$ can induce structure in peptides of this type.

**Role of the Density of Positive Charges and Their Spatial Distribution.** In the first design (Figure 5A, peptide 1), two neighboring rows (row C and F) were filled with eight arginine residues in order to form positive interactions with the silica surface upon formation of a helix. The interaction with the silica surface could depend on the precise spatial distribution of the positive charges and on how densely they are situated. Therefore, three peptides (peptides 2, 3, and 4) that differed in these respects were investigated. Two peptides were produced in which the total number of positive charges were reduced to 4 (compared with peptide 1) by replacing 4 of the arginine residues with other amino acid residues. In peptide 2, the arginine residues in row F were replaced with asparagine residues, which should result in a helix with one straight row that contains 4 arginine residues. In peptide 3, the arginine residues in positions 6, 10, 20, and 24 were replaced by asparagine residues resulting in a remaining zigzag pattern with 4 arginine residues. The other rows were not changed. The number of positive charges in peptide 4 was increased to 12 by removing 4 glutamine residues in order to introduce a third row of arginine residues. In all of these peptides, the charge on the "solution side" of the helix was maintained at −3 by three glutamic acid residues. The increase of positive charges might provide a larger interaction surface for the peptide once a helix was formed.

The results in Table 2 and Figure 4 clearly show that the amount of formed helix upon binding to the nanoparticles is strongly dependent on both the density and the spatial distribution of positive charges on the side of the helix that faces the silica surface. The comparison of peptides 1, 2, 3, and 4 demonstrates that the helical content is positively correlated to the charge density. Peptides 1 and 4 (8 and 12 arginine residues, respectively) have equally high tendencies to form a helix, while peptides 2 and 3 (4 arginine residues each) have the weakest tendency to form helices. Notably, the difference in helical content between peptides with 8 and 12 positive charges is minimal, whereas the helical content in the free peptide is notably lower in the peptide with 12 arginines indicating that, for a design with switch-like properties, it is favorable to have a large number of arginines.

Comparison of peptides 2 and 3, which both have 4 differently distributed arginine residues (a straight row and a zigzag pattern, respectively), indicates that the spatial distribution of arginines influences the tendency to form a helix at suboptimal concentrations of positive charges. Therefore, arginines that form a straight row in the helix are more efficient than a zigzag pattern.

**Effects of Replacing Arginine with Lysine and the Coupling to Effects of pH.** In the peptides already discussed,

**Table 2.** Calculated Percentage of Helicity of All Peptides in the Presence and Absence of Silica Nanoparticles and the Difference between Them, at All Three pH Levels Used in This Investigation

| | 9.8 | | | 9.0 | | | 8.4 | | |
|---|---|---|---|---|---|---|---|---|---|
| | Particles | Free | Δ | Particles | Free | Δ | Particles | Free | Δ |
| Peptide 1 | 41 | 7 | 34 | 39 | 8 | 31 | 36 | 4 | 32 |
| Peptide 2 | 22 | 4 | 18 | 25 | 5 | 20 | 21 | 5 | 16 |
| Peptide 3 | 16 | 5 | 11 | 15 | 4 | 11 | 15 | 4 | 11 |
| Peptide 4 | 42 | 2 | 40 | 37 | 3 | 34 | 36 | 5 | 31 |
| Peptide 5 | 35 | 4 | 31 | 24 | 3 | 21 | 24 | 3 | 21 |
| Peptide 6 | 41 | 5 | 36 | 24 | 4 | 20 | 20 | 4 | 16 |
| Peptide 7 | 16 | 7 | 9 | 20 | 4 | 16 | 16 | 3 | 13 |
| Peptide 8 | 34 | 7 | 27 | 34 | 4 | 30 | 30 | 6 | 24 |
| Peptide 9 | 48 | 5 | 43 | 39 | 7 | 32 | 39 | 4 | 35 |
| Peptide 10 | 24 | 4 | 20 | 22 | 5 | 17 | 18 | 4 | 14 |
| Peptide 11 | 58 | 16 | 42 | 54 | 19 | 35 | 52 | 7 | 45 |
| Peptide 12 | 56 | 4 | 52 | 54 | 5 | 49 | 60 | 4 | 56 |

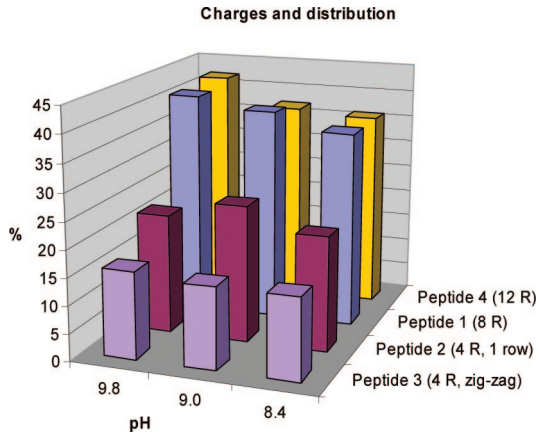


**Figure 4.** Induced helical content in arginine (R) containing peptides showing the dependence on the number of positive charges and their distribution.

arginine residues have been used as the positively charged anchor in the helix formation on the nanoparticle. In peptide 5 (Table 1 and Figure 5B), lysine residues replace the 8 arginine residues in rows C and F of peptide 1. A comparison (Table 2, Figure 6) of peptide l with peptide 5, where both have 8 positive charges in the interaction area, shows a much lower helical content with lysine residues at pH 8.4 and 9.0. At pH 9.8, the difference in helical content is much smaller. Notably, arginine residues are more efficient than lysine in forming electrostatic interactions with the silica surface under conditions in which the negative charges are sparsely distributed. Specifically, the delocalized positive charge on the guanidinium group seems to have a higher chance of finding a corresponding negative charge on silica than the more localized positive charge on the lysine amino group. Consequently, when the charge density on the silica surface is increased by increasing the pH, the lysine residue finds an interaction partner more easily, and the difference with arginine in helix formation efficiency become smaller. Notably, lysine has a high helix propensity above its p$K_a$, indicating that the loss of a positive charge by increased pH or by finding a negative charge on the silica can both contribute to helix formation. Regardless of the detailed understanding of these factors, it is clear that arginine residues should be used in the design of peptides that form helices on silica surfaces. A comparison of the effects of different pH on induction of helix shows small effects with no obvious trend when all peptides are compared. Notably, the density of negative charges on the surface increases from 0.5 $OH^-/nm^2$ at pH 8.4 to 0.7 $OH^-/nm^2$ at pH 9 and 1.1 $OH^-/nm^2$ at pH 9.8. A corresponding doubling in the charge density in the peptide (from 4 to 8 arginines in peptide 2 and peptide 1, respectively) result in an approximate doubling of the helical content at all pH. Thus, it seems as if a charge density of 0.5 $OH^-/nm^2$ on the nanoparticle is sufficient for formation of the required electrostatic interactions at all charge densities in arginine-containing peptides

**Importance of the Helix-Forming Propensities of Glutamine and Glutamic Acid.** In peptide 1, rows A, D, and E, which extend out from the particle surface toward the solution, were filled with glutamine (row D and row E) and glutamic acid (row A). These amino acid residues were selected because they provide a polar surface facing the solution, and the glutamic acid residues were chosen because their negative charge would be repelled by the silica surface, which might aid in orienting the helix on the surface. They were selected in favor of asparagine and aspartic acid because they have higher helix-forming propensities,[33] which might contribute to stabilizing the helix on the surface. In order to test the importance of the helix-forming propensities, a peptide (peptide 6, Figure 5C) was synthesized where asparagine and aspartic acid residues replaced glutamine and glutamic acid residues, respectively. By introducing aspartic acids and asparagines, which are both more common in "loops" and "turns", the net charge of the peptide is preserved. A comparison between peptide 1 and peptide 6 (Table 2, Figure 7) shows that, although both show a decrease in helical content with decreasing pH, the peptides containing asparagine and aspartic acid have a falloff much greater than the parent peptide (no. 1). Thus, the helix-forming propensities of glutamine and glutamic acid residues play a major role in stabilizing the surface-bound helix at lower pH (8.4 and 9.0) levels. At higher pH (e.g., pH 9.8), it appears as if other factors are dominant.

**Importance of Charged Residues on the Solution-Exposed Side of the Bound Peptide.** The importance of orienting the helix on the surface, by introducing negative charges on the side that points away from the silica surface and faces the solution, was tested by investigating peptides

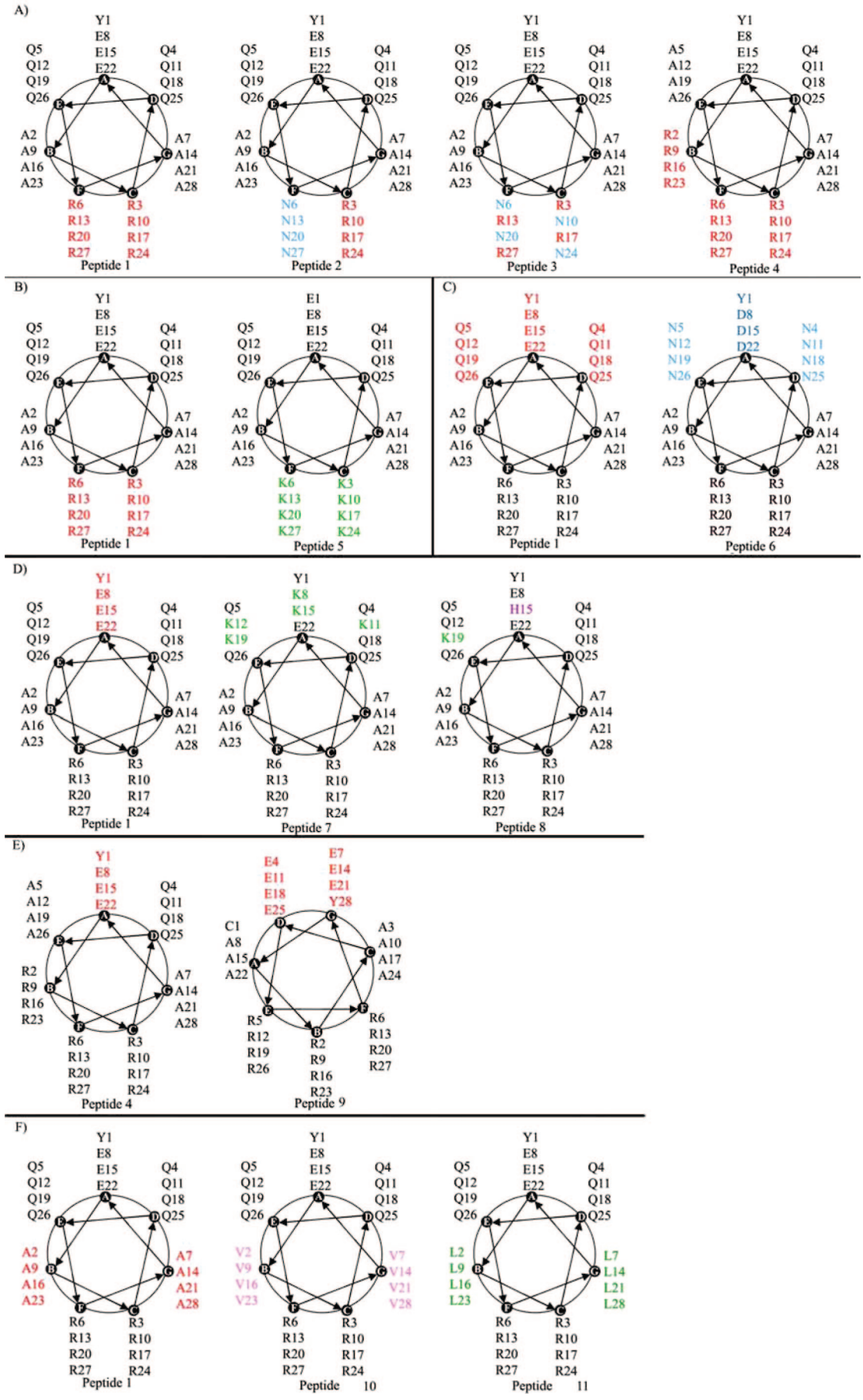


**Figure 5.** Comparison of investigated peptide designs with differences highlighted in color.

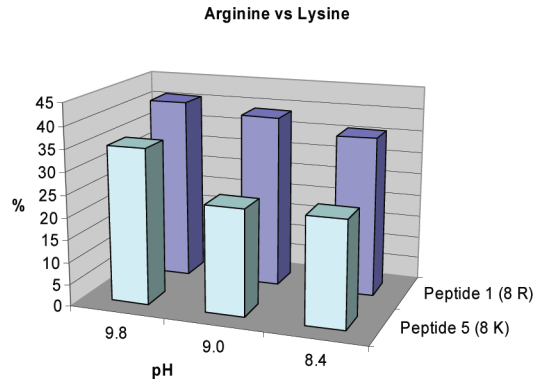


**Figure 6.** Efficiency of arginine (R) or lysine (K) residues to induce helical structure.

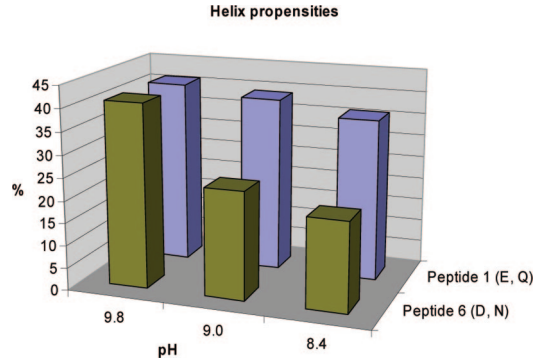


**Figure 7.** Effect of helix-forming propensities in the polar part of the peptide on induced helicity. Dependence of the constituting amino acids, i.e. replacing glutamic acid (E) and glutamine (Q) with aspartic acid (D) and asparagine (N), respectively.

1, 4, 7, 8, and 9 (Figure 5D and E). The original peptide 1 contains 3 glutamic acid residues, leading to a total charge of −3 on the solution face, and a total net charge on the peptide of +5. In peptide 7, two glutamic acids, at positions 8 and 15, and three glutamines, at positions 11, 12, and 19, were replaced with lysine thereby altering the net charge from −3 to +3 on the solution face and giving a total net charge of the peptide of +8. Peptide 8 contains a histidine in position 15 and a lysine in position 19 providing the peptide with a net negative charge at the solution face of −1 and a total net charge of +7. Peptide 4 contains 3 glutamic acid residues giving a charge of −3 on the solution face and a total net charge of +9, since peptide 4 contains 12 arginines. To further compare the effect the charges have on the helical formation, peptide 9 was synthesized containing 12 arginine residues and 2 rows of glutamic acid and another row of glutamine was discarded, giving a charge of −7 on the solution side and a total charge of +5 (Figure 5E). A peptide (no. 7) with a net charge of +3 on the solution face forms only a small amount of helix upon addition of nanoparticles (Figure 8a). Altering the net charge on the solution face from +3 to −1 causes an increase in helicity from ∼16% to ∼34%, thereby doubling the amount of helix formed. Further increase of the net negative charge from −1 to −3 on the solution face results in a 5−7% increase in helical content. A comparison of the two peptides containing 12 arginines but with an increase of the net negative charge from −3 to −7 gives a minor increase in helicity (Figure 8b). Considered together, these results show that the presence of negatively charged residues on the solution face of the helix contributes favorably to helical structure formation. Notably, the repulsion between the negative charges on the silica surface and the negatively charged amino acid residues on the solution face of the helix contributes to an efficient induction and stabilization of a bound helix.

**Role of Hydrophobic Residues on the "Sides" of the Helix.** Alanine-rich sequences are often used when designing helix-forming peptides since alanine have a high helix propensity,[34] and the side-chain is too small to induce unwanted aggregation due to hydrophobic interactions.[35] Most of the peptides investigated in this study contain alanine residues in rows B and G. To illuminate the role of alanine residues in helix stabilization and to investigate the influence of hydrophobic residues in these positions, peptides 10 and 11 were synthesized. The alanine residues were replaced with valine residues in peptide 10 and with leucine residues in peptide 11 (Figure 5F), respectively. The leucine residues would increase the hydrophobicity on the "sides" of the helix and essentially retain the propensity to form helix. The introduction of valine residues would also increase hydrophobicity on the "sides" of the helix. However, valine has a much lower propensity to form a helix than alanine and leucine.

The replacement of the alanine residues with valine residues reduces the ability to form helical structures on the particle surface. Noticeably, the bulky valine side chains stabilize peptide conformations that are not compatible with productive interactions with the particles or for the efficient formation of a helix.

Introducing leucine instead of alanine (peptide 11) has a great effect on the helicity, which increases by almost 20% (Table 2, Figure 9). The increased stabilization through hydrophobic interactions, presumably with neighboring peptides, appears to work favorably for the formation of helices on the surface. Hence, it is apparent that helix propensity is important, and when amino acids have a comparable propensity, the hydrophobicity plays a large role.

On the downside, from the viewpoint of using the nanoparticle as an "all or none" switch, replacing alanine with leucine also increases the amount of helix formed in the absence of particles (Table 2).

**Effect of the Twist in the Helical Backbone—Optimizing the Design.** The present results from the studies of peptides 1 to 11 have shown important aspects of the design. A high number of positive charges in the interaction area favor helix formation and the positive charges should emanate from arginine. It was shown that alanine is favored in comparison with leucine, having much less helix in the absence of nanoparticles. It was also shown that the net negative charge on the solution-facing side of the peptide should be high. It is also favorable to use glutamic acid and glutamine in comparison with aspartic acid and asparagine because of their differences in helix-forming propensity.

Until now, all peptides investigated have been based on a design where the constituting amino acids are placed in the

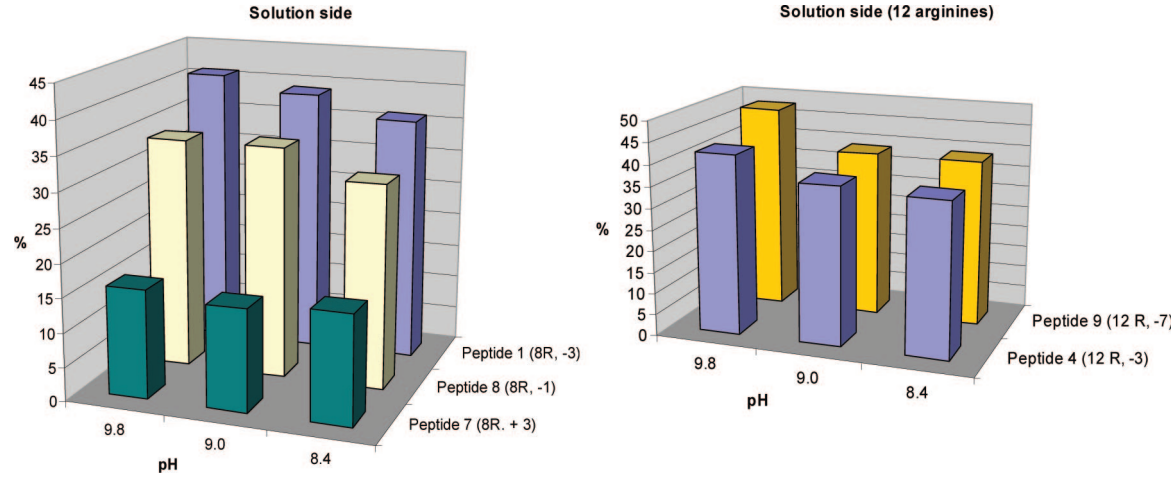


**Figure 8.** Induced helicity, considering both total charge and distribution of charges. To the left, peptides containing 8 arginines and, to the right, peptides containing 12 arginines both with a variation of total charge on the solution facing side.

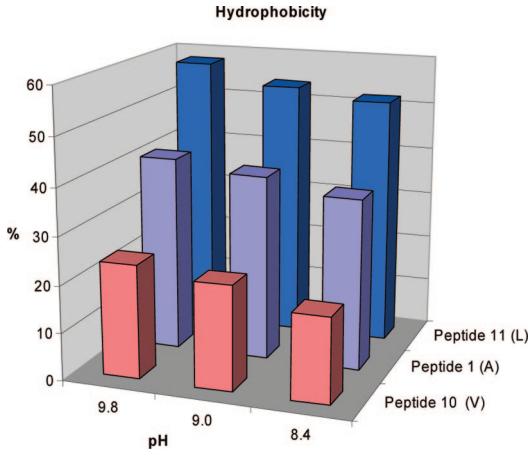


**Figure 9.** Influence of hydrophobicity, coupled to the propensity, on the formation of helix at the silica surface. V = valine, A = alanine, and L = leucine.

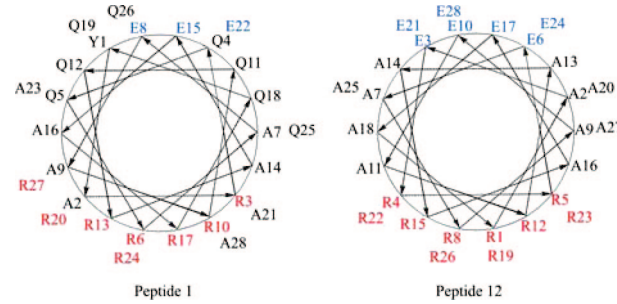


**Figure 10.** Helical wheel of peptide 1 and 12 with a proper 100° twist between residues. Positive amino acids are colored in red, and negative are colored in blue.

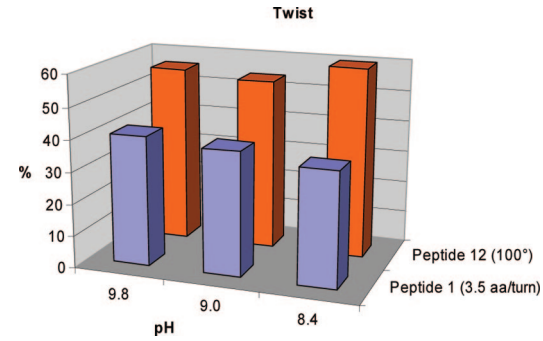


**Figure 11.** Effect on the formation of helix when helical twist has been taken into consideration.

fixed rows of the helical wheel. This type of visualization (which approximate each helical turn with 3.5 amino acid residues) makes the helix easier to conceptualize but does not take into consideration that every turn in the helix consists of 3.6 amino acids. In the design of peptide 12, the knowledge from the above analysis was used, and in addition, each residue was located with the proper 100° angular difference. Thus, the design of peptide 12 incorporates an increase of positive charge from +8 to +10 on the interaction face (compared with the original peptide 1). The arginine residues in peptide 12 also occur in a more restricted segment of the helical wheel. The number of negative charges on the face toward the solution increased from 3 to 7, and they are distributed in a slightly larger segment of the wheel. The "sides" of the helix were filled with alanine residues because of their high helix-forming propensity. Inspection of Figure 10 shows that the helix has a focused distribution of charges and there are no overlaps between amino acid residues that have different design properties. As is shown by the comparison with peptide 1 in Figure 11, this optimized peptide has the highest helical content, in the nanoparticle complex, out of all of the investigated peptides, and the optimization process has resulted in a substantial increase in helical content.

Since this work aims at developing peptides with the ability to bind to nanoparticles, it is important to achieve a high binding strength; therefore, the binding of the optimized peptide and two "reference" peptides to the nanoparticles was measured by use of isothermal titration calorimetry. The dissociation constants were determined, and no correlation between induced helicity and binding strength was found, nor did the number of positive charges correlate to binding strength. Interestingly, it was found that binding of the optimized peptide (peptide 12, $K_d = 7 \times 10^{-6}$ M) to the nanoparticles is saturated at 9 to 10 peptides per nanoparticle with no sign of aggregation upon further addition of peptide

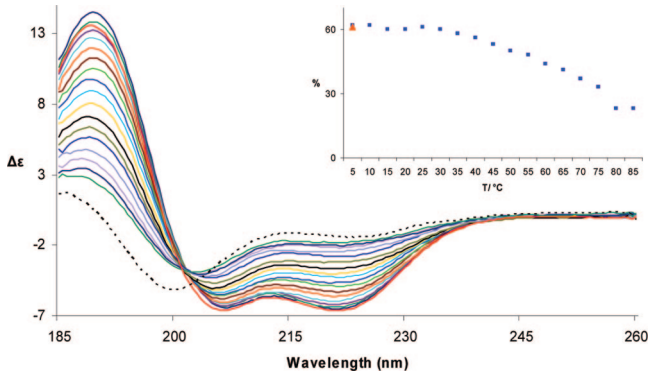


**Figure 12.** CD spectra of the dependence of the helical content on temperature for peptide 12 at pH 9 in presence of 9 nm particles. The dashed line shows a typical spectrum of the peptide in absence of particles. The inset shows the calculated percentage of helix at each temperature, going from 62% at 5 °C to 23% at 85 °C, where the orange triangle represents the subsequent cooling.

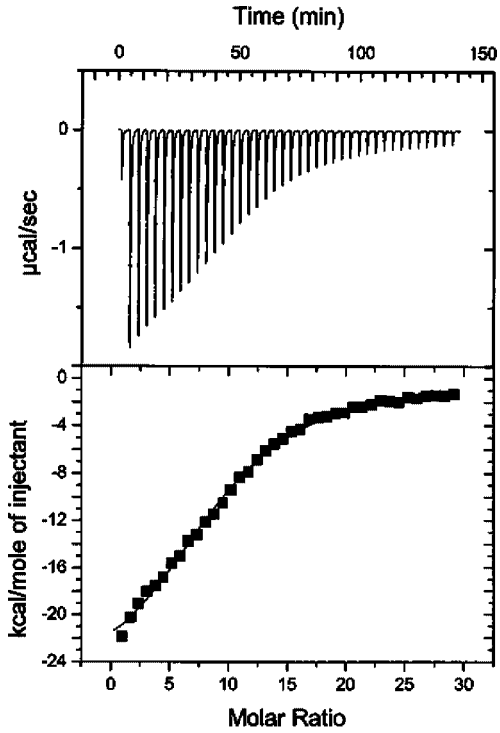


**Figure 13.** Titration of peptide 12 into a solution of 2.5 $\mu$M nanoparticles monitored by isothermal titration calorimetry. Evaluation by a one site model gives, $N = 9.2 \pm 0.1$ and $K_d = 6.6 \pm 0.3$ $\mu$M.

(see Figure 12). The other investigated peptides (peptide 11, $K_d = 19 \times 10^{-6}$ and peptide 6, $K_d = 3 \times 10^{-6}$) are saturated at 7 peptides per nanoparticle, and further addition of peptide give results that indicate aggregation (data not shown). Apparently, the optimized design not only gives rise to the highest induced helicity but also hinders formation of unwanted aggregation. In a second experiment the temperature dependence on the induced helicity was investigated. It was found that the induced helix is remarkably stable at high temperatures; the helical content is maintained at a constant level between 5 and 35 °C and is only halved at 75 °C (Figure 13). Further, it is apparent that the loss in helicity upon heating is fully reversible as the original amount of helix is observed once the sample has been cooled to 5 °C after heating.

**Conclusions.** From a systematic variation of the amino acid composition in the designed peptides, it has been shown that the ability to form a helical structure upon binding to the silica surface is dominated by two factors. First, the helical content is strongly correlated to the net positive charge on the side of the helix that interacts with the silica, and arginine residues are strongly favored over lysine residues in these positions. The second important factor is to have a high net negative charge on the side of the helix that faces the solution. It appears that both attractive and repulsive electrostatic forces dominate the induction and stabilization of a bound helix. It is also evident that using amino acids that have a high propensity to form a helix in solution is also advantageous for helix formation on surfaces. Thus, it is possible to design a peptide that has a very low helical content when free in solution (4%) but that adopts a well-defined helix when interacting with silica nanoparticles (60%).

**Acknowledgment.** This work was supported by a grant from the Swedish National Science Research Council to B.-H.J. (K5104-5999) and by a grant from the Knut and Alice Wallenberg Foundation to K.B. P.N. is enrolled in the graduate school Forum Scientium and the Biomimetic Materials Science program, both supported by the Swedish Foundation for Strategic Research (SSF). The silica particles were kindly provided by EKA Chemicals, Stenungsund, Sweden.

## References

(1) Yao, S.; Ghosh, I.; Zutshi, R.; Chmielewski, J. *Angewandte Chemie-International Edition* **1998**, *37* (4), 478–481.
(2) Yao, S.; Ghosh, I.; Zutshi, R.; Chmielewski, J. *Nature* **1998**, *396* (6710), 447–450.
(3) Johnsson, K.; Allemann, R. K.; Widmer, H.; Benner, S. A. *Nature* **1993**, *365* (6446), 530–532.
(4) Severin, K.; Lee, D. H.; Kennan, A. J.; Ghadiri, M. R. *Nature* **1997**, *389* (6652), 706–709.
(5) Lee, D. H.; Granja, J. R.; Martinez, J. A.; Severin, K.; Ghadiri, M. R. *Nature* **1996**, *382* (6591), 525–528.
(6) Talanian, R. V.; McKnight, C. J.; Kim, P. S. *Science* **1990**, *249* (4970), 769–771.
(7) O'Neil, K. T.; Hoess, R. H.; DeGrado, W. F. *Science* **1990**, *249* (4970), 774–778.
(8) Billsten, P.; Freskgård, P. O.; Carlsson, U.; Jonsson, B. H.; Elwing, H. *FEBS Lett.* **1997**, *402* (1), 67–72.
(9) Karlsson, M.; Carlsson, U. *Biophys. J.* **2005**, *88*, 3536–3544.
(10) Karlsson, M.; Mårtensson, L. G.; Jonsson, B. H.; Carlsson, U. *Langmuir* **2000**, *16* (22), 8470–8479.
(11) Lundqvist, M.; Andresen, C.; Christensson, S.; Johansson, S.; Karlsson, M.; Broo, K.; Jonsson, B. H. *Langmuir* **2005**, *21*, 11903–11906.
(12) Lundqvist, M.; Sethson, I.; Jonsson, B. H. *Langmuir* **2004**, *20*, 10639–10647.
(13) Lundqvist, M.; Sethson, I.; Jonsson, B. H. *Biochemistry* **2005**, *44* (30), 10093–10099.
(14) Lundqvist, M.; Sethson, I.; Jonsson, B. H. *Langmuir* **2005**, *21* (13), 5974–5979.
(15) Baron, M. H.; Revault, M.; Servagent-Noinville, S.; Abadie, J.; Quiquampoix, H. *J. Colloid Interface Sci.* **1999**, *214* (2), 319–332.
(16) Billsten, P.; Carlsson, U.; Jonsson, B. H.; Olofsson, G.; Höök, F.; Elwing, H. *Langmuir* **1999**, *15* (19), 6395–6399.

(17) Billsten, P.; Wahlgren, M.; Arnebrant, T.; McGuire, J.; Elwing, H. *J. Colloid Interface Sci.* **1995**, *175* (1), 77–82.
(18) Bower, C. K.; Xu, Q.; McGuire, J. *Biotechnol. Bioeng.* **1998**, *58* (6), 658–662.
(19) Buijs, J.; Hlady, V. *J. Colloid Interface Sci.* **1997**, *190* (1), 171–181.
(20) Giacomelli, C. E.; Bremer, M. G. E. G.; Norde, W. *J. Colloid Interface Sci.* **1999**, *220* (1), 13–23.
(21) Larsericsdotter, H.; Oscarsson, S.; Buijs, J. *J. Colloid Interface Sci.* **2001**, *237* (1), 98–103.
(22) Maste, M. C. L.; Norde, W.; Visser, A. J. W. G. *J. Colloid Interface Sci.* **1997**, *196* (2), 224–230.
(23) Lundqvist, M.; Nygren, P.; Jonsson, B. H.; Broo, K. *Angewandte Chemie-International Edition* **2006**, *45* (48), 8169–8173.
(24) Fillon, Y; Verma, A.; Ghosh, P.; Ernenwein, D.; Rotello, V. M.; Chmielewski, J. *J. Am. Chem. Soc.* **2007**, *129* (21), 6676+.
(25) Capriotti, L. A.; Beebe, T. P.; Schneider, J. P. *J. Am. Chem. Soc.* **2007**, *129* (16), 5281–5287.
(26) Sonnefeld, J. *J. Colloid Interface Sci.* **1996**, *183* (2), 597–599.
(27) Anthonycahill, S. J.; Benfield, P. A.; Fairman, R.; Wasserman, Z. R.; Brenner, S. L.; Stafford, W. F.; Altenbach, C.; Hubbell, W. L.; Degrado, W. F. *Science* **1992**, *255* (5047), 979–983.
(28) Lobley, A.; Whitmore, L.; Wallace, B. A. *Bioinformatics* **2002**, *18* (1), 211–212.
(29) Whitmore, L.; Wallace, B. A. *Nucleic Acids Res.* **2004**, *32*, W668–W673.
(30) Compton, L. A.; Johnson, W. C. *Anal. Biochem.* **1986**, *155* (1), 155–167.
(31) Manavalan, P.; Johnson, W. C. *Anal. Biochem.* **1987**, *167* (1), 76–85.
(32) Sreerama, N.; Woody, R. W. *Anal. Biochem.* **2000**, *287* (2), 252–260.
(33) Chou, P. Y.; Fasman, G. D. *Biochemistry* **1974**, *13* (2), 211–222.
(34) Doig, A. J.; Baldwin, R. L. *Protein Sci.* **1995**, *4* (7), 1325–1336.
(35) Liu, J.; Zheng, Q.; Deng, Y. Q.; Cheng, C. S.; Kallenbach, N. R.; Lu, M. *Proc. Natl. Acad. Sci. U.S.A.* **2006**, *103* (42), 15457–15462.

NL080386S